QUANTUM RESONANCES: LINE PROFILES AND DYNAMICS

Ivana PAIDAROVÁ[a,*] and Philippe DURAND[b]

[a] *J. Heyrovský Institute of Physical Chemistry, Academy of Sciences of the Czech Republic, Dolejškova 8, CZ-182 23 Prague 8, Czech Republic; e-mail: ivana.paidarova@jh-inst.cas.cz*

[b] *Laboratoire de Physique Quantique, IRSAMC, Unité Associée au CNRS no 505, Université Paul Sabatier, 31062 Toulouse Cedex 4, France; e-mail: philippe.durand@irsamc.ups-tlse.fr*

Received August 3, 2002
Accepted October 14, 2002

Dedicated to Professors Petr Čársky, Ivan Hubač and Miroslav Urban on the occasion of their 60th birthdays.

The wave operator theory of quantum dynamics is reviewed and applied to the study of line profiles and to the determination of the dynamics of interacting resonances. Energy-dependent and energy-independent effective Hamiltonians are investigated. The q-reversal effect in spectroscopy is interpreted in terms of interfering Fano profiles. The dynamics of an hydrogen atom subjected to a strong static electric field is revisited.

Keywords: Green function; Wave operator; Effective Hamiltonian; Quantum resonance; q-Reversal effect; Hydrogen atom.

In this tribute paper we aim to review some recent developments in the theory of quantum resonances which are ubiquitous in many domains of chemistry and spectroscopy. Since resonances are localized in molecules, they can be investigated by quantum chemistry methods analogous to the methods developed for bound states. Whenever physics requires simultaneous determination of several almost degenerate states, the Bloch theory based on wave operators and effective Hamiltonians is the most appropriate[1,2]. Wave operators generalize the concept of wave function by treating several states on an equal footing. Effective Hamiltonians provide a finite number of exact energies for stationary (bound) states. For resonances (quasi-bound states), effective Hamiltonians contain spectroscopical (line profiles) and dynamic information (*e.g.*, an exponential decay for an isolated resonance).

In the following, first the basic concepts of wave operator and effective Hamiltonian are reviewed. Then an exactly solvable model, which describes several interacting resonances decaying into several continua, is presented.

It is shown that a simple two-dimensional effective Hamiltonian gives access to the most basic profiles in spectroscopy. Finally, the dynamics of ionization of an hydrogen atom subjected to a strong static electric field is investigated.

THEORY

The wave operator approach of quantum dynamics[3] focuses on relevant quasi-bound states. These quasi-bound states, localized in atoms and molecules, may be described by atomic and molecular orbitals in the same way as if they were true bound states. An important characteristic of our approach is that it fully exploits the rigidity properties of analytical functions and especially of analytical continuation, which play a key role in the theory of resonances[4]. Partitioning techniques and perturbative approaches play a fundamental role in the theory that generalizes schemes which were previously developed for bound states[5].

We assume that n quasi-bound states, which may be resonances, are relevant for investigating line profiles and the dynamics of the resonances within an energy range of interest. The quasi-bound states $|i\rangle$ (i = 1, 2, ..., n) span an n-dimensional space, the so called *model (or inner) space*, whose projector is

$$P_0 = \sum_{i=1}^{n} |i\rangle\langle i|, \qquad \langle i|j\rangle = \delta_{ij}, \qquad i = 1, 2, \ldots, n. \tag{1}$$

The projector onto the *complementary (or outer) space* is Q_0 ($P_0 + Q_0 = 1$). For any initial state belonging to the model space, the full dynamical information is contained in the resolvent projected, on the right, in the model space:

$$\frac{1}{z - H} P_0 = \Omega(z) \frac{P_0}{z - H^{\text{eff}}(z)}. \tag{2}$$

Equation (*2*) defines the wave operator $\Omega(z)$ and the effective Hamiltonian $H^{\text{eff}}(z)$. H is the Hamiltonian of the system and z means the energy extended in the complex plane. Formal exact expressions of the wave operator and of the effective Hamiltonian are

$$\Omega(z) = P_0 + \frac{Q_0}{z - H} H P_0 \quad \text{and} \quad H^{\text{eff}}(z) = P_0 H \Omega(z). \tag{3}$$

Hereafter, resolvents such as $1/(z - H)$ or $Q_0/(z - H)$ are unambiguously defined for Im $z > 0$ and are assumed to be analytically continued in the second Riemann sheet for Im $z < 0$. The effective Hamiltonian is also currently expressed as

$$H^{\text{eff}}(z) = P_0 H P_0 + R(z), \qquad R(z) = P_0 H \frac{Q_0}{z - H} H P_0 . \tag{4}$$

$R(z)$ defines an energy-shift operator[6]. Multiplying both sides of Eq. (*2*), on the left, by P_0 and using the intermediate normalization [$P_0 = P_0\Omega(z)$] results in

$$P_0 \frac{1}{z - H} P_0 = \frac{P_0}{z - H^{\text{eff}}(z)} . \tag{5}$$

The energy-dependent effective Hamiltonian $H^{\text{eff}}(z)$, which appears in Eqs (*2*), (*3*) and (*5*) plays a central role in the theory. The aim of the theory is to provide effective Hamiltonians which depend as little as possible on the energy. This can be achieved by extending the model space. In addition, model Hamiltonians describing several resonances decaying into several decay channels provide exact effective Hamiltonians which may describe realistic situations. The lineshapes (or line profiles) are characterized by the intensity

$$I(E) = -\frac{1}{\pi} \text{Im}\, G(E), \qquad G(E) = \langle \phi | \frac{P_0}{E - H^{\text{eff}}(E)} | \phi \rangle . \tag{6}$$

E is the energy on the real axis. It is assumed in Eq. (*6*) that the system was prepared at the initial time $t = 0$ in the state $|\phi\rangle$ belonging to the model space. The lineshape is normalized to unity:

$$\int_{-\infty}^{\infty} I(E)\, \mathrm{d}E = 1. \tag{7}$$

The knowledge of the effective Hamiltonian provides the dynamics in the model space, which can be recovered by the inverse Laplace transformation. The projection in the model space of the time-dependent wave function is given by

$$|\phi(t)\rangle = \frac{1}{2\pi \mathrm{i}} \int_C \frac{P_0}{z - H^{\text{eff}}(z)} |\phi\rangle e^{-\mathrm{i}zt/\hbar}\, \mathrm{d}z . \tag{8}$$

The integration path C in the complex plane runs on the real-energy axis from $+\infty$ to $-\infty$ and is closed in the lower part (Im $z < 0$). The probability of remaining in the initial state (survival probability) at time t is

$$P(t) = |\langle\phi|\phi(t)\rangle|^2 . \qquad (9)$$

More generally, the probability of passing from $|\phi\rangle$ at initial time $t = 0$ to any final state $|\phi_f\rangle$ belonging to the model space at time t is given by

$$P_f(t) = |\langle\phi_f|\phi(t)\rangle|^2 . \qquad (10)$$

Equations (*6*), (*8*), (*9*), and (*10*) show that the spectroscopical and dynamical observables can be derived from the knowledge of the energy-dependent effective Hamiltonian. If the model space is large enough, the effective Hamiltonian may depend weakly on the energy. It is especially interesting to consider exactly solvable models, which yield exact energy-independent effective Hamiltonians and "exact dynamics" in the sense that will be precised later. Moreover, these models give a clear description and an understanding of line profiles in spectroscopy. Hereafter, we will denote by H^{eff} an effective Hamiltonian which does not depend on the energy. Its spectral resolution

$$H^{\text{eff}} = \sum_{i=1}^{n} \mathcal{E}_i |\phi_i)(\phi_i| , \qquad \mathcal{E}_i = E_i - \frac{\mathrm{i}}{2}\Gamma_i \qquad (11)$$

allows to express the observables in terms of simple expressions. For example, Eqs (*6*) and (*9*) become

$$I(E) = -\frac{1}{\pi}\operatorname{Im} G(E) , \qquad G(E) = \sum_{i=1}^{n} \frac{f_i}{E - \mathcal{E}_i} , \qquad f_i = \langle\phi|\phi_i)(\phi_i|\phi\rangle \qquad (12)$$

and

$$P(t) = \left| \sum_{i=1}^{n} f_i \exp\left(-\mathrm{i}\frac{\mathcal{E}_i}{\hbar} t\right) \right|^2 . \qquad (13)$$

The f_i's are generalized oscillator strengths. They are dimensionless complex numbers which characterize the transitions between the initial state $|\phi\rangle$ and the states $|\phi_i)$. In Eqs (*11*) and (*12*), the notation $|\phi_i)$ refer to the symmetric scalar product[7]. For more details, see ref.[8]

RESULTS AND DISCUSSION

An Exactly Solvable Model

We consider a model system implying several resonances or quasi-bound states decaying into several decay channels. The model generalizes the original Fano model[9] and other models which discretize the continuum[6,10,11]. These *discrete* model Hamiltonians are closely related to *continuous* models, which were initially introduced in nuclear physics[12,13]. All these models are efficient for investigating line profiles and irreversible evolutions. However, there are many advantages to start from quasi-continua instead of continua. The mathematics is simpler because one remains inside the Hilbert space of square-integrable functions. In addition, it is possible to determine exact expressions of the effective Hamiltonians. Finally, the properties of the continua can be recovered when the energy spacings of the quasi-continua tend to zero[6].

The model describes n quasi-bound states interacting with m quasi-continua. The quasi-bound states $|i\rangle$ (i = 1, 2, ..., n) span the model space. The orthonormalized states $|ka\rangle$ (a = 1, 2, ..., m) define the complementary (outer) space whose projector is

$$Q_0 = \sum_{k,a} |ka\rangle\langle ka|, \qquad \langle ka|k'b\rangle = \delta_{kk'}\delta_{ab} ;$$

$$k, k' = 0, \pm 1, \pm 2, \ldots \quad \text{and} \quad a, b = 1, 2, \ldots, m.$$

Henceforth, the indexes a, b, ... will characterize the quasi-continua (decay channels). The matrix representation of the model Hamiltonian H in the basis of the states $|i\rangle$ (inner space) and of the states $|ka\rangle$ (outer space) is given in Fig. 1. Inside the model space, the off diagonal matrix elements are denoted $H_{ij} = \langle i|H|j\rangle$ and the diagonal terms $E_i^0 = \langle i|H|i\rangle$. The matrix representation of the Hamiltonian is diagonal in the outer space. The energy of the state $|ka\rangle$ is $k\delta_a$. The energies of the quasi-continua extend from $-\infty$ to $+\infty$

($k = 0, \pm1, \pm2, \ldots$), δ_a is the energy spacing between the neighboring levels in channel a. Note that the couplings between the inner space and the quasi-continua $v_i^a = \langle ka|H|i\rangle$ ($i = 1, 2, \ldots, n$; $a = 1, 2, \ldots, m$) do not depend on the index k which would label the energy in a continuous model. Since the matrix representation of the model Hamiltonian is diagonal in the outer space, the effective Hamiltonian (*3*) can be easily calculated. The use of the summation formula

$$\sum_{k\in Z}(z-k)^{-1} = \frac{\pi}{\tan \pi z}\,, \qquad Z = \{0, \pm 1, \pm 2, \ldots\}$$

leads to the exact equation

$$H^{\text{eff}}(z) = \hat{H} - \frac{\mathrm{i}}{2}\hat{\Gamma}(z)\,. \tag{14}$$

$\hat{H} = P_0 H P_0$ is the projection of H into the model space. No couplings between the quasi-continua are considered in this model and hence the dissipative part of $H^{\text{eff}}(z)$ can be expressed as a sum over the channels:

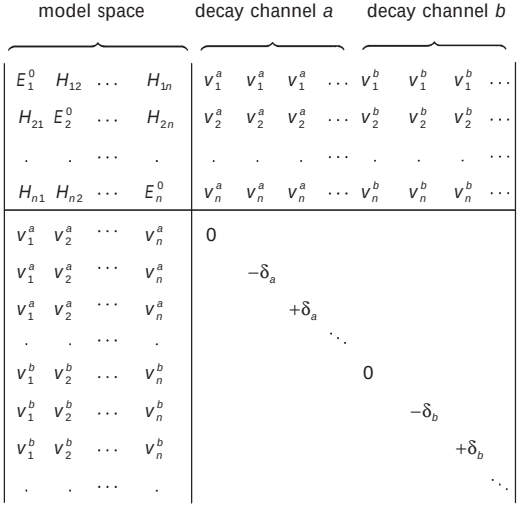

FIG. 1

Matrix representation of the model Hamiltonian in the basis of the quasi-bound states (n-dimensional model space) and of the states of m decay channels labeled a, b, ... (outer space). Note that the matrix is diagonal in the outer space and that the couplings between the model space and the outer space are constant within each decay channel

$$\hat{\Gamma}(z) = \sum_{a=1}^{m} \hat{\Gamma}_a(z), \qquad \hat{\Gamma}_a(z) = 2\pi |V_a\rangle\langle V_a| \times \mathrm{i}\cot\left(\frac{\pi z}{\delta_a}\right). \tag{15}$$

$\hat{\Gamma}_a(z)$ characterizes the dissipation in channel *a*. The vector $|V_a\rangle$ collects the couplings between the inner space and the outer space indexed by *a*:

$$|V_a\rangle = \sum_{i=1}^{n} V_i^a |i\rangle, \qquad V_i^a = \frac{1}{\sqrt{\delta_a}} v_i^a . \tag{16}$$

If all the energy spacings have the same value δ, Eq. (*15*) becomes simpler

$$\hat{\Gamma}(z) = \hat{\Gamma} \times \mathrm{i}\cot\left(\frac{\pi z}{\delta}\right), \qquad \hat{\Gamma} = \sum_{a=1}^{m} \hat{\Gamma}_a, \qquad \hat{\Gamma}_a = 2\pi |V_a\rangle\langle V_a| . \tag{17}$$

Equations (*14*) and (*15*) are exact but, as expected, energy-dependent. Let us now derive from the energy-dependent effective Hamiltonian an energy-independent effective Hamiltonian which can be considered as exact as specified below.

The periodic expression in Eq. (*15*) can be expanded in Fourier series in the complex plane (Im $z > 0$):

$$\mathrm{i}\cot\left(\frac{\pi z}{\delta}\right) = 1 + 2\sum_{k=1}^{\infty} \exp\left(\mathrm{i}\frac{2\pi k z}{\delta}\right). \tag{18}$$

Using Eq. (*18*) and retaining only the first term on the right-hand side transforms Eq. (*14*) into

$$H^{\mathrm{eff}} = \hat{H} - \frac{\mathrm{i}}{2}\hat{\Gamma} , \tag{19}$$

where

$$\hat{\Gamma} = 2\pi \sum_{a=1}^{m} |V_a\rangle\langle V_a| . \tag{20}$$

The effective Hamiltonian (*19*) is energy-independent. It provides the exact dynamics for times shorter than $\tau = 2\pi\hbar/\delta$ (ref.[3]) (all the energy spacings of the continua are assumed to have the same value δ). Since τ can be arbitrarily increased by decreasing δ, we can consider that the effective Hamiltonian

(*19*) is exact. The dissipative Hamiltonian (Eq. (*19*)) can also be derived from a continuous model[12,13]. The direct relationship between the matrix elements of the model Hamiltonian and the dissipative operators (Eq. (*20*)) expands the list of the advantages starting from a discrete model Hamiltonian. The amplitudes of the dissipative operators are of paramount importance for discussing the interference phenomena arising from the couplings between the resonances and the decay channels. When there is only one decay channel, the dissipative operator (Eq. (*20*)) can be written in the form

$$\hat{\Gamma} = 2\pi |V\rangle\langle V| , \qquad (21)$$

where the index labeling the channel has been suppressed. $\Gamma = 2\pi\langle V|V\rangle$ is the only non-zero eigenvalue of $\hat{\Gamma}$ (ref.[14]). The rank = 1 property is not an artifact of the model and remains true when the discrete-continuum coupling becomes energy dependent (see, *e.g.*, ref.[13], p. 372).

Effective Hamiltonian

For the sake of clarity, we will use boldface letters for the matrix representations of the operators acting in the model space. The matrix representation of the effective Hamiltonian (Eq. (*19*)) reads

$$\mathbf{H}^{\text{eff}} = \mathbf{H} - \frac{\mathrm{i}}{2}\mathbf{\Gamma} . \qquad (22)$$

The components of $\mathbf{H}$ and $\mathbf{\Gamma}$ in the basis $\{|i\rangle\}$ are

$$H_{ij} = \langle i|H|j\rangle , \qquad \Gamma_{ij} = 2\pi\sum_{a=1}^{m} V_i^a \, V_j^a , \qquad i, j = 1,\ 2,\ \ldots,\ n . \qquad (23)$$

We also denote

$$E_i^0 = H_{ii} , \qquad i = 1,\ 2,\ \ldots,\ n , \qquad (24)$$

the zero-order energies of the quasi-bound states $|i\rangle$. Equation (*23*) makes clear that changes in the signs of the matrix elements coupling the model space and the outer space may produce significant changes of the line-

shapes and of the dynamics (see Fig. 7 discussed in Subsection Trapping Effect). In Eq. (*23*) the constraints associated with a unique decay channel appear clearly through the product structure of the matrix elements of **Γ**. If the matrix elements of **Γ** are small with respect to those of **H**, reversible evolutions prevail. On the contrary, if the matrix elements of **Γ** dominate those of **H**, irreversible evolutions may occur associated with the formation of fast and slow decay modes. The formation of fast and slow decay modes in open systems is quite generic[14].

The aim of the next paragraphs is to show that the exactly solvable model Hamiltonian describes the most fundamental characteristics of lineshapes and simultaneously exact dynamics. Already the smallest model space (n = 2) provides many generic results. We will investigate processes decaying mainly into one decay channel (m = 1), which exhibit the most extended interference effects[15,16].

The matrix representation of the effective Hamiltonian in the basis of two quasi-bound states (n = 2) decaying into one continuum (m = 1) is written in the form

$$\mathbf{H}^{\mathrm{eff}} = \begin{bmatrix} E_1^0 & v \\ v & E_2^0 \end{bmatrix} - \frac{\mathrm{i}}{2}\begin{bmatrix} \Gamma_{11} & \sqrt{\Gamma_{11}\,\Gamma_{22}} \\ \sqrt{\Gamma_{11}\,\Gamma_{22}} & \Gamma_{22} \end{bmatrix}, \qquad (25)$$

where E_1^0 and E_2^0 are the zero-order energies of the two quasi-bound states. The coupling term v is real. We assume that the couplings between the quasi-bound states and the quasi-continuum are real and have the same sign. The eigenvalues of **Γ** are 0 and $\Gamma_{11} + \Gamma_{22}$ and the components of the corresponding eigenvectors are $[\sqrt{\Gamma_{22}}, -\sqrt{\Gamma_{11}}]$ and $[\sqrt{\Gamma_{11}}, \sqrt{\Gamma_{22}}]$, respectively. This system was previously studied by many authors[17–19]. Nevertheless, its reexamination is justified. Many papers focused on the trajectories of the energies in the complex plane whereas our work is oriented toward lineshapes, survival and transition probabilities.

Two Interacting Resonances

The first example (Fig. 2) is freely inspired by a recent study of two interfering vibrational resonances in the van der Waals molecule $I_2\cdots Ne$ decaying into several vibrational channels[20]. The parameters of the effective Hamiltonian (*25*) are given in the caption of Fig. 2. The molecule is assumed to be prepared in the state

$$|\phi\rangle = \cos\theta\,|1\rangle + \sin\theta\,|2\rangle\,. \qquad (26)$$

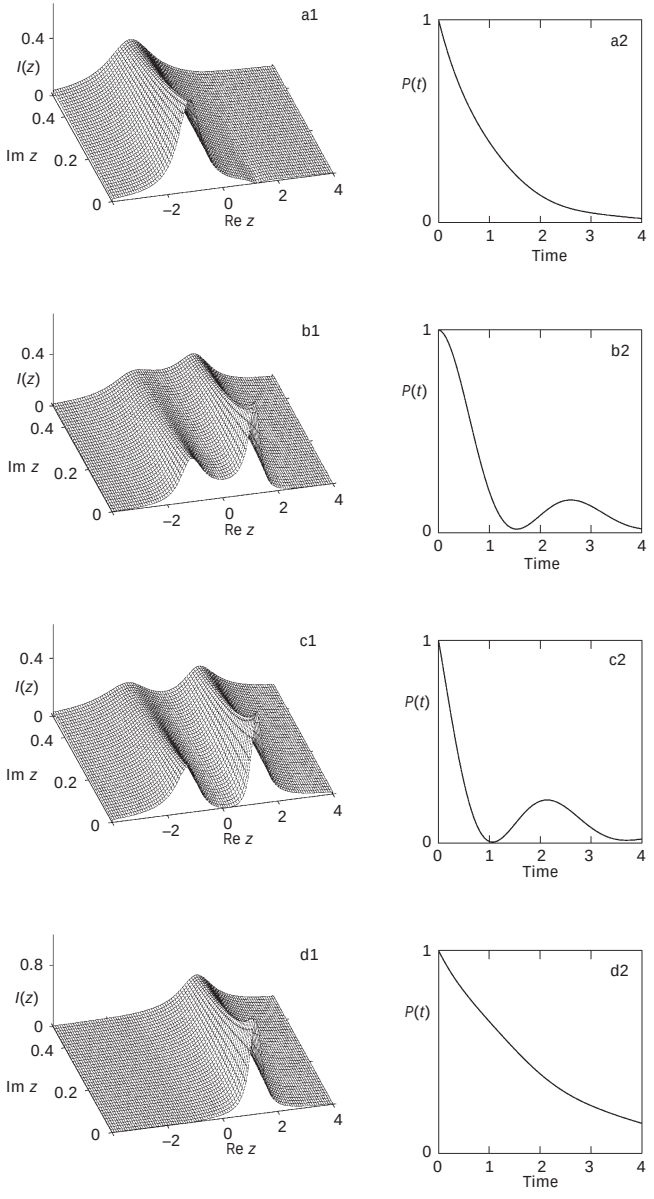

FIG. 2.

Two interacting resonances. The effective Hamiltonian is given by Eq. (*25*). $E_1^0 = -1.25$, $E_2^0 = 1.25$, $v = 0$, $\Gamma_{11} = 1$, and $\Gamma_{22} = 0.5$. The lineshapes $I(E)$ (Eq. (*6*)) (on the real energy axis) and the survival probabilities $P(t)$ (Eq. (*9*)) are represented for four initial states $|\phi\rangle = \cos\theta\,|1\rangle + \sin\theta\,|2\rangle$. a $\theta = 0$, b $\theta = \pi/4$, c $\theta = -\pi/4$, and d $\theta = \pi/2$ (arbitrary units)

$|1\rangle$ and $|2\rangle$ describe two resonances which are directly coupled to the continuum. We have represented in Fig. 2 the line profiles $I(E)$ (Eq. (*6*)) (on the left) and the survival probabilities $P(t)$ (Eq. (*9*)) (on the right) for the values $\theta = 0$, $\pi/4$, $-\pi/4$, and $\pi/2$. Instead of plotting $I(E)$ on the real energy axis, as it is usual, we have represented the surfaces corresponding to $I(z)$ in the complex plane for Im $z > 0$. This representation highlights the role of analyticity which is essential in our approach. Note that the surfaces $I(z)$ are smooth for Im $z >> 0$. This means that the useful information concerning the resonances is to be found in the complex plane for Im $(z) > 0$ as it is implicit in Eq. (*17*). In cases a and d in Fig. 2 ($\theta = 0$ and $\theta = \pi/2$), pure resonances were prepared at the initial time. The Breit–Wigner profiles a1 and d1 give birth to the exponential decays a2 and d2. In cases b and c ($\theta = \pm\pi/4$) the two resonances add and subtract their amplitudes and produce damped oscillations near the critical regime.

The effective Hamiltonian (*25*) with the parameters $E_1^0 = E_2^0 = 0$, $v = 0.5$, $\Gamma_{11} = 0$, and $\Gamma_{22} = \Gamma$ models a resonance indirectly coupled to one continuum. Figure 3 illustrates various dynamic regimes, $|\phi\rangle = |1\rangle$ being the initial state. The coupling term v is kept constant while Γ increases from 0.2 in case a to 6 in case c. The extreme situations are in cases a and c. In case a there are two narrow resonances a1 and damped Rabi oscillations a2. The occupation probabilities plotted in a2 clearly indicate that, in this case, the resonance and the quasi-bound state directly coupled to the decay channel participate in the dynamics. In case c we get the Breit–Wigner profile c1 and the exponential decay c2. Case b corresponds to the critical regime ($\Gamma = 4v$). Note the transitory occupation in b2 of the second quasi-bound state directly coupled to the continuum (dotted lines).

Fano Profiles

Fano profiles are ubiquitous in many areas of atomic and molecular spectroscopy. Universality of these profiles suggests that they should be described within a unique comprehensive theory. Fano profile results from the interference of a discrete state (resonance) and a continuum. The asymmetry of the profiles comes from the dependence on energy of the coupling between the discrete state and the continuum[21]. We have recently shown that Fano profiles can be described in terms of interference between two quasi-bound states[8]. The first is the discrete state and the second models the relevant part of the continuum (doorway state, see ref.[12], p. 179). Here we present an illustrative example. The discrete state and the continuum are modeled by the two states $|1\rangle$ and $|2\rangle$ which span the model space. The

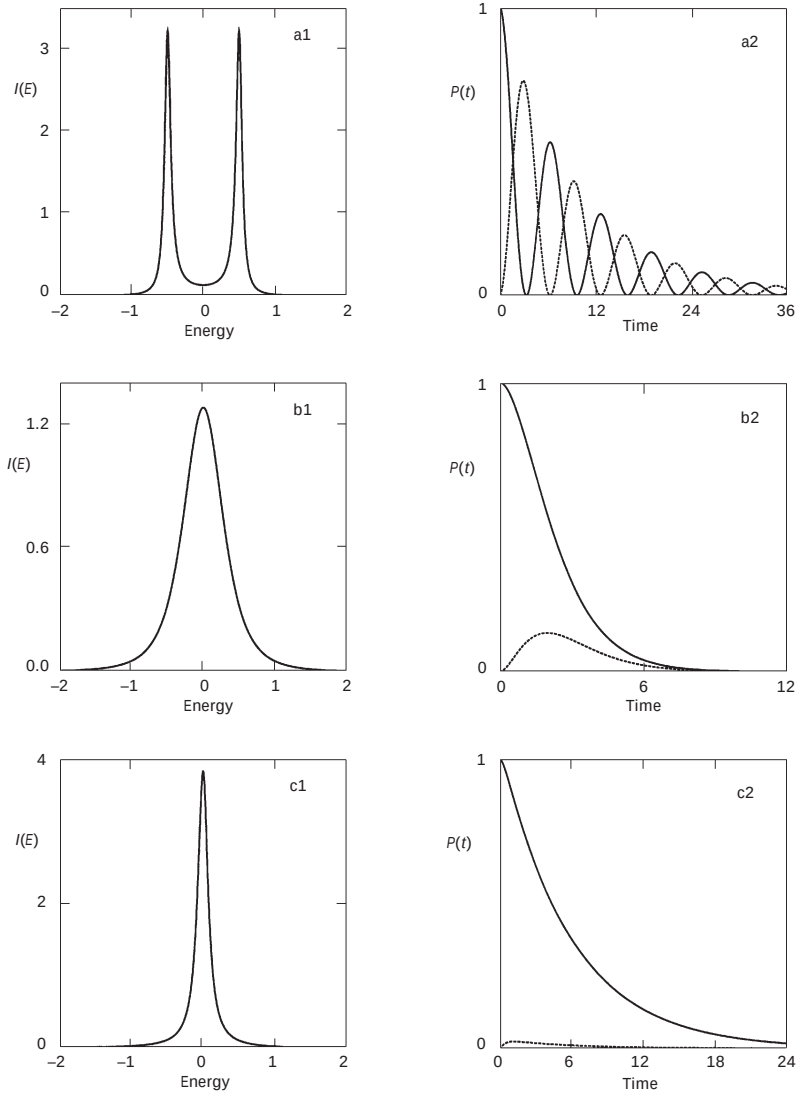

FIG. 3

From weak to strong coupling (Rabi oscillations). The effective Hamiltonian is given by Eq. (*25*). $E_1^0 = E_2^0 = 0$, $v = 0.5$, $\Gamma_{11} = 0$, and $\Gamma_{22} = \Gamma$. The lineshapes (on the left) and the dynamics (on the right) are presented for three values of Γ. a $\Gamma = 0.2$, b $\Gamma = 2$ and c $\Gamma = 6$. In all the cases the system is prepared in the initial state $|1\rangle$. In a2, b2 and c2, the full lines correspond to the survival probability of the initial state $|1\rangle$ and the dotted lines to the occupation probability of the quasi-bound state $|2\rangle$ (arbitrary units)

system is described by the effective Hamiltonian (Eq. (*25*)). Figure 4 shows the lineshapes (on the left) and the survival probabilities (on the right) obtained by varying the initial state. The excitation of the continuum, represented by $|2\rangle$, increases from a to c (see the caption of Fig. 4). a1 and b1 display typical Breit–Wigner and Fano profiles while destructive interference still remains in case c when only the continuum is excited. A more detailed description of our approach to Fano profiles is given in ref.[8], and generalized expressions of Fano profiles can be found in ref.[22]

q-Reversal Effect

The aim of this paragraph is to provide a simple model for describing and understanding the fundamentals of the q-reversal effect[23]. We consider three interfering quasi-bound states (n = 3) decaying into a unique continuum (m = 1). In the basis of the three quasi-bound states the matrix representation of the effective Hamiltonian is written in the form

$$\mathbf{H}^{\text{eff}} = \begin{bmatrix} E_1^0 & . & . \\ H_{21} & E_2^0 & . \\ H_{31} & H_{32} & E_3^0 \end{bmatrix} - \frac{\mathrm{i}}{2} \begin{bmatrix} \Gamma_{11} & . & . \\ \sqrt{\Gamma_{22}\,\Gamma_{11}} & \Gamma_{22} & . \\ \sqrt{\Gamma_{33}\,\Gamma_{11}} & \sqrt{\Gamma_{33}\,\Gamma_{22}} & \Gamma_{33} \end{bmatrix}. \qquad (27)$$

For the sake of simplicity the upper part of the real symmetric matrices in Eq. (*27*) has not been represented. E_1^0 (i = 1, 2, 3) are the zero-order energies of the quasi-bound states $|i\rangle$ of partial widths $\Gamma_{ii} = 2\pi V_i^2$ (see Eq. (*23*)). V_i is a component of the coupling vector $|V_a\rangle$ (Eq. (*16*)). The index a was suppressed because there is only one decay channel. The V_i's are assumed to be real and positive.

The resonances $|1\rangle$ and $|2\rangle$ and the quasi-bound state $|3\rangle$ describing the relevant part of the continuum span a three-dimensional model space (n = 3). The parameters of the effective Hamiltonian are given in the caption of Fig. 5. In order to excite selectively the resonances obtained by diagonalization of the effective Hamiltonian, the initial state was chosen successively in the form

$$|\phi_{++}\rangle = \mathcal{N}\mathrm{Re}[c(\ \ |\phi_1\rangle + |\phi_2\rangle) + |\phi_3\rangle]$$

$$|\phi_{+-}\rangle = \mathcal{N}\mathrm{Re}[c(\ \ |\phi_1\rangle - |\phi_2\rangle) + |\phi_3\rangle]$$

$$|\phi_{-+}\rangle = \mathcal{N}\mathrm{Re}[c(-|\phi_1\rangle + |\phi_2\rangle) + |\phi_3\rangle]$$

$$|\phi_{--}\rangle = \mathcal{N}\mathrm{Re}[c(-|\phi_1\rangle - |\phi_2\rangle) + |\phi_3\rangle] \qquad (28)$$

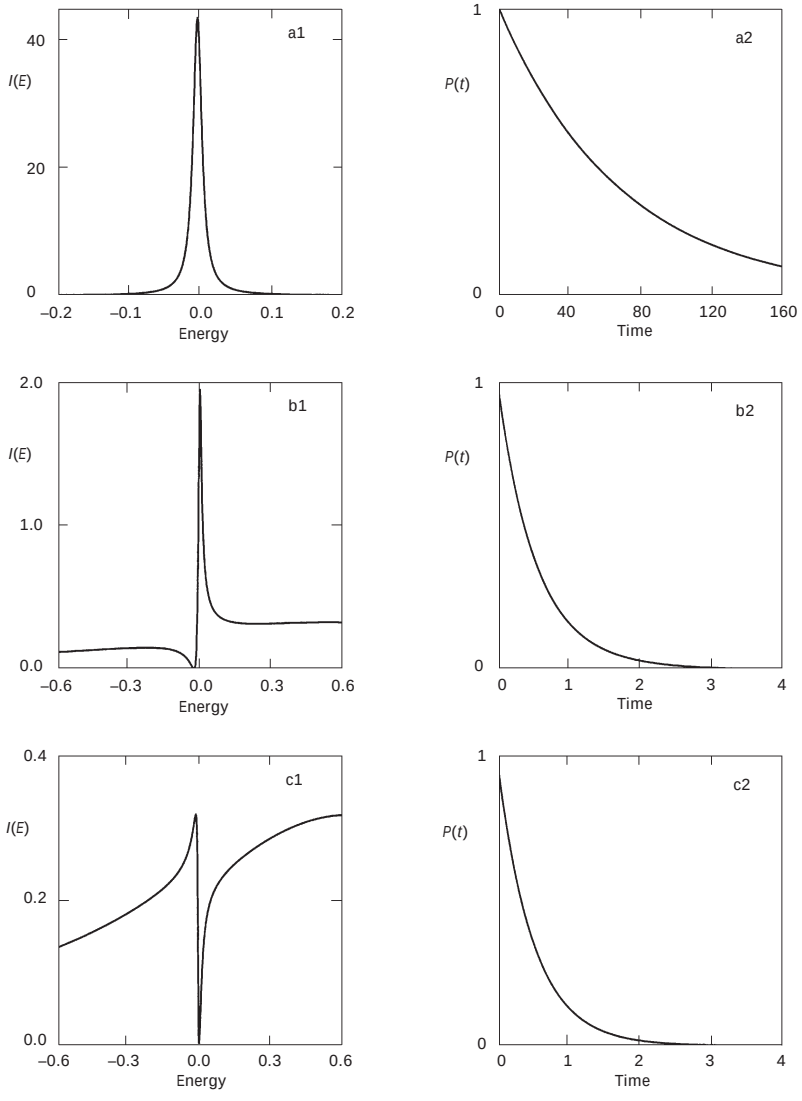

FIG. 4

Fano profiles. The effective Hamiltonian ($n = 2$) is given by Eq. (*25*). $E_1^0 = 0.0$, $E_2^0 = 0.6$, $v = 0.1$, $\Gamma_{11} = 0$, and $\Gamma_{22} = 2$. The lineshapes (on the left) and the dynamics (on the right) are presented for the system prepared in the initial states a $|\phi\rangle = |1\rangle$, b $|\phi\rangle = 0.24(|1\rangle + 4|2\rangle)$ and c $|\phi\rangle = |2\rangle$ (arbitrary units)

where $|\phi_1\rangle$, $|\phi_2\rangle$ and $|\phi_3\rangle$ are the eigenstates of $\mathbf{H}^{\text{eff}}$ and $\mathcal{N}$ is a normalization factor. In all the cases $c = 0.1$. Figure 5 indicates clearly that the q-reversal effect described in ref.[23] can be understood in terms of constructive and destructive interferences between the resonances and the continuum. This straightforward interpretation of the q-reversal effect in terms of resonances interfering with a short-lived state generalizes our description of Fano profiles resulting from interferences between a resonance and a quasi-bound state of larger width[8]. Our approach based on the superposition principle of states is simpler and more comprehensive than the methods based on the analysis of the phase shifts of asymptotic states.

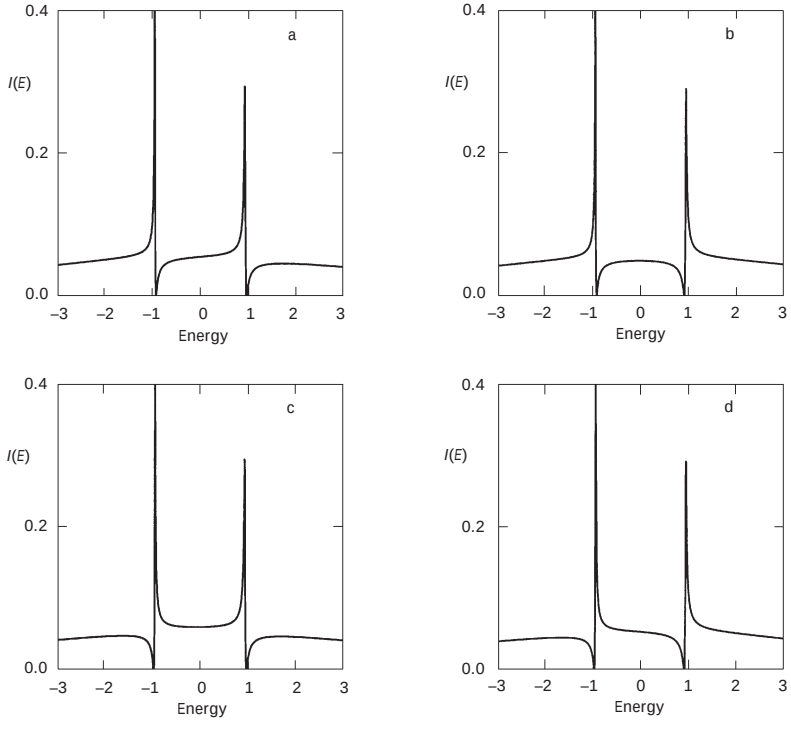

FIG. 5

q-Reversal effect (lineshapes). The hermitian part of the effective Hamiltonian (Eq. (*27*)) is diagonal: $E_1^0 = -1$, $E_2^0 = 1$ and $E_3^0 = 0$. The resonances $|1\rangle$ and $|2\rangle$ are weakly coupled to the continuum ($\Gamma_{11} = 0.5$ and $\Gamma_{22} = 0.8$) whereas the short-lived quasi-bound state $|3\rangle$ is strongly coupled to the continuum ($\Gamma_{33} = 10$). The lineshapes $I(E)$ (Eq. (*6*)) represented in a, b, c, and d correspond, respectively, to the initial states ϕ_{++}, ϕ_{+-}, ϕ_{-+}, and ϕ_{--} (Eq. (*28*)) (arbitrary units)

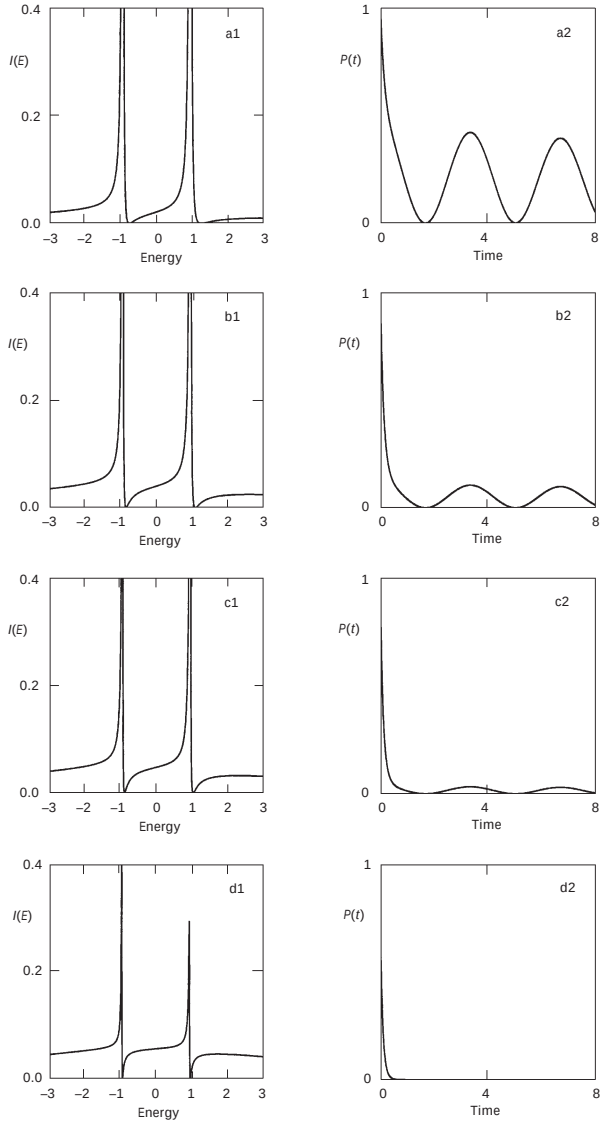

FIG. 6

q-Reversal effect (lineshapes and survival probabilities). The parameters of the effective Hamiltonian (Eq. (*27*)) are the same as in Fig. 5. The lineshapes $I(E)$ (Eq. (*6*)) and the survival probabilities $P(t)$ (Eq. (*9*)) are represented for the initial state $|\phi\rangle = \mathcal{N}(\mathrm{Re}[0.1(|\phi_1\rangle + |\phi_2\rangle) + \lambda|\phi_3\rangle]$. a $\lambda = 0.1$, b $\lambda = 0.2$, c $\lambda = 0.3$, and d $\lambda = 1$. The survival probabilities $P(t)$ show a continuous evolution from reversible oscillations in a2 to an irreversible decay in d2 by increasing the excitation of the continuum (arbitrary units)

Figure 6 shows the evolution of the lineshape and of the associated survival probability by increasing the initial excitation of the "continuum" $|\phi_3\rangle$. The system is prepared in the state $|\phi\rangle = \mathcal{N}(\mathrm{Re}[0.1(|\phi_1\rangle + |\phi_2\rangle) + \lambda|\phi_3\rangle]$. The values of the parameter λ are 0.1, 0.2, 0.3, and 1, respectively, in a, b, c, and d. Although the lineshapes are similar in all cases, the dynamical regimes look quite different. By increasing the excitation of the continuum (from a to d) one passes from quasi-reversible Rabi-like oscillations in a2 to dynamical regimes which become more and more irreversible.

Trapping Effect

The signs of the couplings between the resonances may be crucial when there are several continua implied in the decay process ($m > 1$). The effective Hamiltonian

$$\mathbf{H}^{\mathrm{eff}} = \begin{bmatrix} 0 & v \\ v & 0 \end{bmatrix} - \frac{\mathrm{i}}{4}\begin{bmatrix} \Gamma & \Gamma \\ \Gamma & \Gamma \end{bmatrix} - \frac{\mathrm{i}}{4}\begin{bmatrix} \Gamma & \pm\Gamma \\ \pm\Gamma & \Gamma \end{bmatrix} \qquad (29)$$

chanel a *chanel b*

describes two interacting resonances ($n = 2$) decaying into two channels labeled *a* and *b* ($m = 2$). For producing nice interference figures, the absolute values of the couplings between the resonances and the continua were chosen identical: $|V_i^a| = |V_i^b| = V_1^a$ ($i = 1, 2$) (see Eq. (*23*) for the Γ_{ij}'s). Changing the sign of one coupling may result in dramatic changes in the lineshapes and in the dynamics. We have investigated two combinations of signs labeled ++ ($V_1^b = V_1^a$, $V_2^b = V_2^a$) and +– ($V_1^b = V_1^a$, $V_2^b = -V_2^a$) which correspond to the dissipative matrices

$$\Gamma_{++} = \begin{bmatrix} \Gamma & \Gamma \\ \Gamma & \Gamma \end{bmatrix} \qquad \text{and} \qquad \Gamma_{+-} = \begin{bmatrix} \Gamma & 0 \\ 0 & \Gamma \end{bmatrix}, \qquad (30)$$

respectively. It is assumed that in both cases the initial state is $|\phi\rangle = |1\rangle$. The results are presented in Fig. 7. In the ++ case, the two continua behave as if there were only one continuum. The eigenvalues of Γ_{++} are 0 and 2Γ which results in a slow and a fast decay mode. As expected, the lineshape a1 exhibits a narrow peak. The survival probability of the state $|1\rangle$ (full line) and the probability of occupation of the state $|2\rangle$ (dotted line), displayed in a2, tend quickly toward a constant after some oscillations. Obviously, for a time much larger than the lifetime of the slow decay mode, these occupa-

tion numbers would tend to zero. In the +– case, Eq. (*30*) indicates that the system can be described in terms of two non-interacting Breit–Wigner resonances. This is clearly seen on the lineshape b1 while the occupation numbers represented in b2 characterize strongly damped oscillations. This means that the value $v = 4$ of the direct coupling between the two resonances is close to the critical regime. Larger values of v would uncouple the two resonances and produce weakly damped Rabi oscillations.

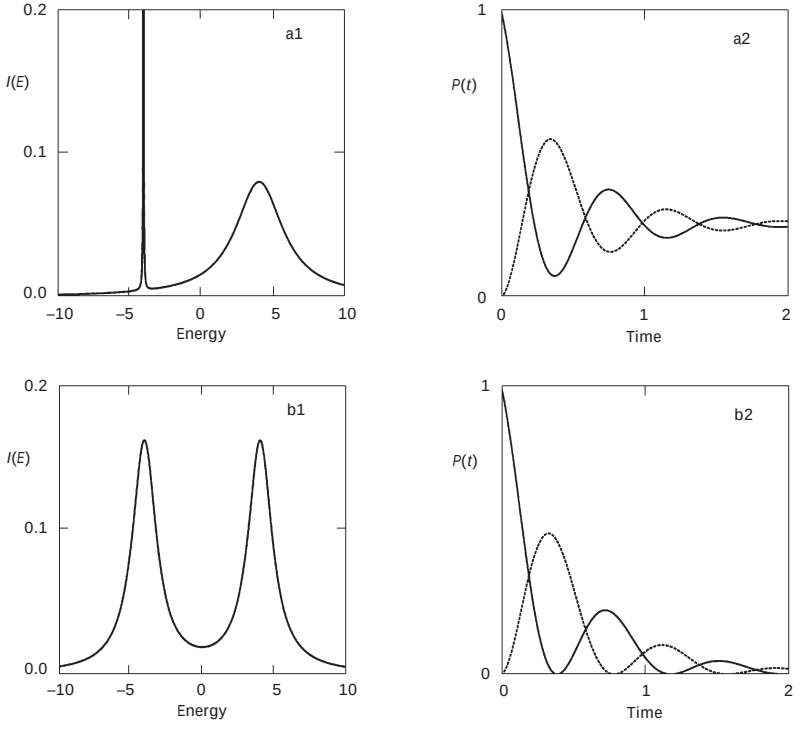

FIG. 7

Fast and slow decay modes (trapping effect). The parameters of the effective Hamiltonian (Eq. (*29*)) are $v = 4$ and $\Gamma = 2$. Two examples of lineshapes and of their associated dynamics are presented for the system prepared in the initial state $|\phi\rangle = |1\rangle$. Plots a1 and a2 arise from the effective Hamiltonian with the dissipative matrix Γ_{++} (Eq. (*30*)). Plots b1 and b2 correspond to the dissipative matrix Γ_{+-} (Eq. (*30*)). The survival probability of the initial state $|1\rangle$ is represented by full lines and the occupation probability of $|2\rangle$ by dotted lines in a2 and b2 (arbitrary units)

Vibronic Dissociation

Two potential energy surfaces S_1 and S_2 generate a double well as shown in Fig. 8. We assume that only the vibrational states of S_2 are coupled with the continuum of states of the dissociative surface S_3. We will show that this quantum system may behave as two weakly coupled oscillators. For the sake of simplicity we consider only two states $|1\rangle$ and $|2\rangle$ in S_1 and two states $|3\rangle$ and $|4\rangle$ in S_2. The parameters of the effective Hamiltonian (*22*) are given in the caption of Fig. 8. At the initial time the system is in the state $|\mathrm{I}\rangle = 1/\sqrt{2}(|1\rangle + |2\rangle)$. The associated lineshape $I(E)$ provides the information concerning the periods of the two normal modes. The survival probability (the kinetic energy remains in S_1) and the transition probability towards the state $|\mathrm{II}\rangle = 1/\sqrt{2}(|3\rangle + |4\rangle)$ (the kinetic energy is transferred in S_2) shows

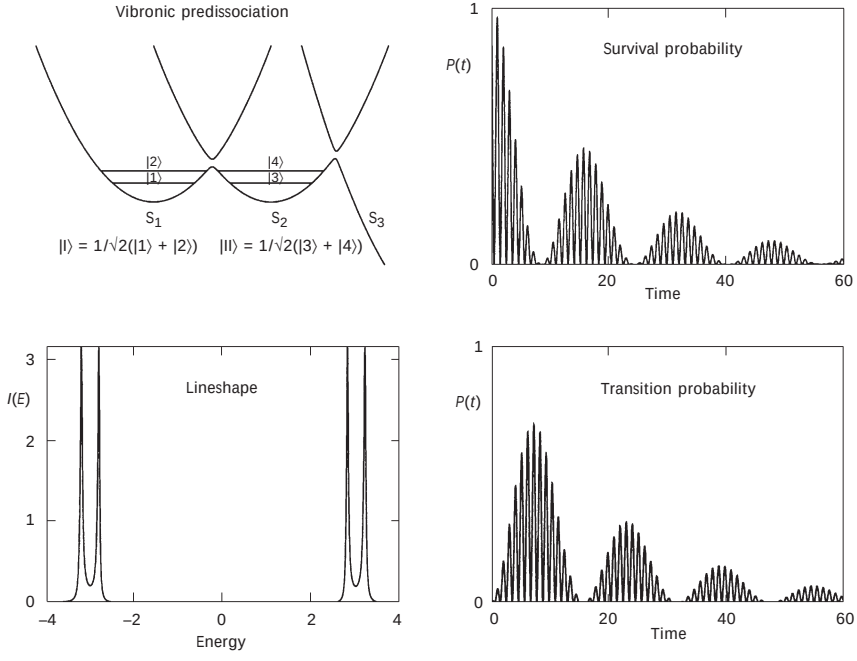

FIG. 8

Vibronic dissociation. The vibrational states $|1\rangle$, $|2\rangle$ (surface S_1) and $|3\rangle$, $|4\rangle$ (surface S_2) generate two weakly coupled oscillators which decay into the continuum associated with the dissociative surface S_3. The zero-order energies of the states are $E_1^0 = E_3^0 = -3$ and $E_2^0 = E_4^0 = 3$. The non-zero off-diagonal terms are $H_{31} = H_{32} = H_{41} = H_{42} = 0.2$. The dissipative part of H^{eff} is characterized by $\Gamma_{11} = \Gamma_{22} = 0$ and $\Gamma_{33} = \Gamma_{44} = 0.1$. The survival probability of the initial state $|\mathrm{I}\rangle = 1/\sqrt{2}(|1\rangle + |2\rangle)$ and the probability of transition towards the state $|\mathrm{II}\rangle = 1/\sqrt{2}(|3\rangle + |4\rangle)$ are represented on the right of the figure (arbitrary units)

the oscillating energy transfer between the two subsystems S_1 and S_2. These oscillations are gradually damped, which corresponds to the dissipation of energy towards the degrees of freedom of the continuum. We have presented a simplified qualitative description of the dynamics without reporting and discussing the complex energies of the effective Hamiltonian. A large number of dynamical regimes could be obtained by varying the parameters of the model. Similar models could be useful for describing the dynamics of reversible and irreversible energy transfer in actual molecules.

Ionization of a Hydrogen Atom Subjected to a Constant Electric Field

We have shown in the previous that an exactly solvable model can provide generic results concerning line profiles and dynamics. The physics was discussed in terms of model spaces and effective Hamiltonians. These concepts are also of fundamental importance for investigating actual systems. Here we consider the simplest one: a hydrogen atom in its ground state subjected to a static electric field. As soon as the atom is subjected to the field, the bound state 1*s* becomes a resonance. For weak fields of amplitude $\mathcal{E} << 0.1$ a.u., ionization is mainly due to the tunneling of the electron through the Coulomb barrier and the survival probability $P(t)$ of the ground state follows approximatively an exponential law. The order of magnitude of the width Γ of the resonance is given approximatively by the quasi-classic theory[24]:

$$P(t) = \exp(-\Gamma t), \qquad \Gamma = \frac{4}{\mathcal{E}} \exp\left(-\frac{2}{3\mathcal{E}}\right). \tag{31}$$

For strong field, $\mathcal{E} > 0.1$ a.u., the decay of the ground state does not follow an exponential law. Surprisingly enough, the full dynamics is still unknown for strong fields. Recently Scrinzi[25] and Geltman[26] have found non-exponential decays which strongly disagree for time $t > 10$ a.u. (see Fig. 4 of ref.[26]). Both authors solved the time-dependent Schrödinger equation using either the standard hermitian Hamiltonian[26] or a non-hermitian complex-scaled Hamiltonian[25]. In order to clarify this disagreement, we have chosen to apply our approach which generalizes the Stark broadening theory (see ref.[26], p. 4770).

Effective Hamiltonian

Our aim is to provide an accurate description of the non-exponential decay of the H atom, initially in the 1*s* state, at any time *t* and especially at $t >> 10$ a.u.

(long-time dynamics). At short time, $t << 10$ a.u., the states mainly implied in the dynamics are the ground state $|1\rangle = 1s$ and the doorway state $|2\rangle = z \times 1s = r \cos\theta \times 1s$ of symmetry p ($l = 1$), which provides the main contribution to the dipolar polarization of the atom ($\alpha = 4$ a.u., the exact value is $\alpha = 4.5$ a.u.). In the basis of the two states $|1\rangle$ and $|2\rangle$, the projector onto the model space is $P_0 = |1\rangle\langle 1| + |2\rangle\langle 2|$ and the energy-dependent effective Hamiltonian can be written in the form

$$\mathbf{H}^{\mathrm{eff}}(z) = \begin{bmatrix} -1/2 & \mathcal{E} \\ \mathcal{E} & R(z) \end{bmatrix}, \qquad R(z) = \langle 2| H \frac{Q_0}{z - H} H|2\rangle . \tag{32}$$

$\mathcal{E}$ is the amplitude of the electric field, $R(z)$ is an energy-shift operator (Eq. (*4*)) and $Q_0 = 1 - P_0$ is the projector onto the complementary space. The inversion of $\mathbf{H}^{\mathrm{eff}}(z)$ provides the exact expression (in a.u.) of the Green function corresponding to the initial state 1*s*:

$$G(z) = \frac{1}{z - E(z)}, \qquad E(z) = -\frac{1}{2} + \frac{\mathcal{E}^2}{z - R(z)} . \tag{33}$$

The diagonalization of the projected hermitian Hamiltonian $Q_0 H Q_0$ was performed in an extended basis of Slater orbitals. For each symmetry l ($l = 0, 1, ..., 9$), ninety Slater orbitals with $n = l + 1, l + 2, ..., l + 90$ and equal exponents $\zeta = 1.1$ were used. The orthogonalization of this set of 900 Slater orbitals and the suppression of the linearly dependent functions led to a basis of 325 orthonormal functions. Using elementary least-square fits, the energy-shift term was approximated by

$$R(z) = \sum_{k=1}^{3} \frac{c_k}{z - e_k}, \qquad \left\{ \begin{array}{l} c_1 = \ 0.058, \ e_1 = -0.232 - \mathrm{i}0.289 \\ c_2 = \ 0.220, \ e_2 = \ 1.942 - \mathrm{i}2.274 \\ c_3 = -0.053, \ e_3 = -0.549 - \mathrm{i}0.545 \end{array} \right\} . \tag{34}$$

Equation (*34*) is approximate but accurate enough to provide short-term and long-term dynamics. Introducing Eq. (*34*) into Eq. (*33*) allows to write $G(z)$ as the ratio of a polynomial of order four to a polynomial of order five:

$$G(z) = P(z)/Q(z) . \tag{35}$$

Dynamics

The Green function along the real energy axis can be written as

$$G(E) = \sum_{k=1}^{5} \frac{f_k}{E - \mathcal{E}_k}\,, \qquad \sum_{k=1}^{5} f_k = 1\,. \tag{36}$$

The complex energies $\mathcal{E}_k$ (k = 1, 2, ..., 5) are the roots of the polynomial $Q(z)$ (Eq. (*35*)) and the f_k's are generalized oscillator strengths. The inverse Laplace transformation provides the survival probability $P(t)$ of the initial state 1*s*:

$$P(t) = \left| \sum_{k=1}^{5} f_k \exp\left(-\mathrm{i} \frac{\mathcal{E}_k}{\hbar} t \right) \right|^2 \tag{37}$$

and the probability of ionization $1 - P(t)$. Equations (*36*) and (*37*) are analogous to Eqs (*12*) and (*13*), which are valid for an energy-independent effective Hamiltonian; in Eqs (*36*) and (*37*) the summation is up to five instead of n = 2 (the dimension of the model space). Here the dependence on the energy is in $R(z)$. Figure 9 shows the survival probability of the ground state of H as a function of time. The agreement between Fig. 9a and the full line curve in Fig. 1 of ref.[25] is almost perfect. This is significant since the calculations were performed by two different approaches: diagonalization of a complex scaled Hamiltonian in ref.[25] and use of a two-dimensional energy-dependent effective Hamiltonian here.

Our approach allows a detailed analysis of the dynamics. The electric field $\mathcal{E}$ = 0.08 a.u. is slightly above the critical value $\mathcal{E}_c$ = 0.0625 a.u. corresponding to the beginning of over-the-barrier ionization. As expected, the long-time dynamics is governed by the dominant pole $\mathcal{E}_1$ = –0.5175 – i0.0023 of the Green function (*36*) whose oscillator strength f_1 = 0.95 – i0.03 is near the value 1 which would lead to an exponential decay. The short-time dynamics (t < 20 a.u.) is mainly due to the next two poles of $G(E)$ of energies $\mathcal{E}_2$ = –0.34 – i0.17 and $\mathcal{E}_3$ = 0.05 – i0.11 whose oscillator strengths are f_2 = 0.04 + i0.02 and f_3 = 0.01 + i0.01, respectively. The oscillator strengths of the other poles are very small and may be neglected. We have investigated the dynamics of the depletion of the H atom in its ground state. However, it would be more realistic to consider that at the initial time the atom is polarized by the electric field. Its wave function derived by perturbation at low field ($\mathcal{E}$ < 0.1 a.u) is approximatively given by $|\phi\rangle = |1\rangle - 2\mathcal{E}|2\rangle$. It is possible to derive the dynamics of the polarized atom

from the effective Hamiltonian (*32*), but this is clearly outside the aim of this study.

It remains to explain the discrepancy between our results, which are almost identical with those of ref.[25], and the strongly oscillating dynamics found in ref.[26]. Note that spurious oscillations (dashed curves) appear at time $t \cong 40$ a.u. in Fig. 1 of ref.[25] when the Hamiltonian is not complex-scaled. No such oscillations appear in our calculation (see the upper-right part of Fig. 9a). This result is reasonable since the ionization of the atom at

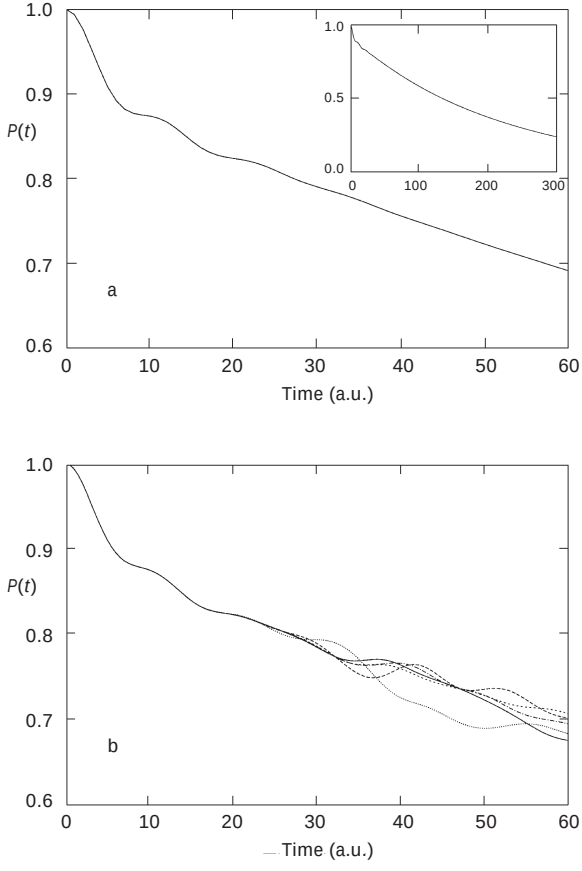

FIG. 9

Decay of the ground state of the hydrogen atom. Survival probability at time t of the ground state of the atom subjected at $t = 0$ to a static electric field of amplitude $\mathcal{E} = 0.08$ a.u.: a Use of the effective Hamiltonian (Eq. (*32*)). b Direct diagonalization of the hermitian Hamiltonian (atom + electric field) using five different basis sets of Slater orbitals. Note the non-exponential decay at short times $t < 20$ a.u. and some spurious oscillations in b at times $t > 40$ a.u. (see the text)

high field is expected to be a strongly irreversible process. We assume that the oscillations in ref.[26] are due to spurious reflections that result from the use of a finite number of square-integrable functions. For checking this hypothesis, we have diagonalized the unscaled hermitian Hamiltonian in several bases of Slater orbitals. The results are represented in Fig. 9b for five basis sets which differ by the number of Slater orbitals (from 600 to 1900) used in the orthogonalization procedure. There is an excellent agreement between the decay laws in plots a and b at $t < 20$ a.u., whereas nonphysical oscillations appear at larger times in b. This result strengthens our hypothesis that the oscillations found in ref.[26] might be artifacts. Numerical experience is that for the dynamics involving several resonances and several time scales, some smoothing or filtering or an averaging procedure is needed. Analytical continuation which is explicit in our approach and implicit in the method of complex scaling do that efficiently.

CONCLUSIONS

In the last fifty years quantum chemistry has developed powerful methods for investigating molecules[27]. Nowadays it is possible to determine accurately many molecular properties, such as bond energies, molecular geometries and spectroscopical constants. The progress has been less systematic for the determination of observables which arise from solutions of the time-dependent Schrödinger equation (*e.g.* line profiles). In all cases the aim of the theory is not only to develop computational codes but also to derive new concepts to describe and understand the chemical and physical phenomena. From that point of view effective Hamiltonians play an important role in many domains of chemistry and spectroscopy. Here we have shown that a simple, exactly solvable model can provide generic results concerning line profiles. The concept of effective Hamiltonians is also useful for actual systems. In this paper an effective Hamiltonian was used for investigating the departure from an exponential decay of the ground state of a hydrogen atom subjected to a strong static electric field. It is worth remarking that a complete treatment of the dynamics applicable at short and long times is still missing.

Finally, the simultaneous study of line profiles and of the dynamics is a nice illustration of the dual role played by the Hamiltonian in quantum mechanics as was frequently underlined by Prigogine[28].

This work was supported by the Grant Agency of the Czech Republic (grants No. 203/00/1025 and No. 203/01/1274).

REFERENCES

1. Lindgren I., Morrison J.: *Atomic Many-Body Theory*, p.184. Springer, Berlin 1982.
2. Durand Ph., Malrieu J.-P. in: *Ab initio Methods in Quantum Chemistry I* (K. P. Lawley, Ed.), p. 352. J. Wiley, New York 1987.
3. Durand Ph., Paidarová I.: *Phys. Rev. A: At., Mol., Opt. Phys.* **1998**, *58*, 1867.
4. Kukulin V. I., Krasnopolsky V. M., Horáček J.: *Theory of Resonances: Principles and Applications*. Academia, Prague 1989.
5. Löwdin P. O.: *J. Chem. Phys.* **1951**, *19*, 1396.
6. Cohen-Tannoudji C., Dupont-Roc J., Grynberg G.: *Atom-Photon Interactions, Basic Processes and Applications*. Wiley, New York 1992. (1st ed.: InterEditions et Editions du CNRS, Paris 1988)
7. Moiseyev N., Certain P. R., Weinhold F.: *Mol. Phys.* **1978**, *36*, 1613.
8. Durand Ph., Paidarová I., Gadéa F. X.: *J. Phys. B: At., Mol. Opt. Phys.* **2001**, *34*, 1953.
9. Fano U.: *Nuovo Cimento* **1935**, *12*, 154.
10. Avan P.: *Thèse*. Université de Paris VI, Paris 1976.
11. Cohen-Tannoudji C., Avan P.: *Atomes et molécules hautement excités*, p. 93. Editions du CNRS, Paris 1977.
12. Mahaux C., Weidenmüller H. A.: *Shell Model Approach to Nuclear Reactions*. North-Holland, Amsterdam 1969.
13. Verbaarschot J. J. M., Weidenmüller H. A., Zirnbauer M. R.: *Phys. Rep.* **1985**, *129*, 369.
14. Desouter-Lecomte M., Jacques V.: *J. Phys. B: At., Mol. Opt. Phys.* **1995**, *28*, 3225.
15. Mies F. H., Krauss M.: *J. Chem. Phys.* **1966**, *45*, 4455.
16. Nitzan A., Jortner J., Berne B. J.: *Mol. Phys.* **1973**, *26*, 281.
17. Friedrich H., Wintgen D.: *Phys. Rev. A: At., Mol., Opt. Phys.* **1985**, *32*, 3231.
18. Müller M., Dittes F.-M., Iskra W., Rotter I.: *Phys. Rev. E: Stat. Phys., Plasmas, Fluids, Relat. Interdiscip. Top.* **1995**, *52*, 5961.
19. von Brentano P.: *Phys. Rep.* **1996**, *264*, 57.
20. Gadéa F. X., Durand Ph., González-Lezana T., Delgado-Barrio G., Villareal P.: *Eur. Phys. J. D* **2001**, *15*, 215.
21. Fano U.: *Phys. Rev.* **1961**, *124*, 1866.
22. Durand Ph., Paidarová I.: *J. Phys. B: At., Mol. Opt. Phys.* **2002**, *35*, 469.
23. Connerade J.-P., Lane A. M.: *Rep. Prog. Phys.* **1988**, *51* 1439.
24. Landau L., Lifshitz E.: *Quantum Mechanics*, p. 257. Pergamon, Oxford 1965.
25. Scrinzi A.: *Phys. Rev. A: At., Mol., Opt. Phys.* **2000**, *61*, 041402.
26. Geltman S.: *J. Phys. B: At., Mol. Opt. Phys.* **2000**, *33*, 4769.
27. Čársky P., Urban M.: *Lect. Notes Chem.* **1980**, 16.
28. Prigogine I.: *From Being to Becoming*, p. 57. Freeman and Company, New York 1980.